Proceedings of the Fourth IASTED International Conference on Signal and Image Processing (SIP),
Kauai, Hawaii, Aug. 12-14, pp. 595-600, 2002.

Application of Affine Transformations for the Co-registration of SPECT Images

Mark A. Rossman[*], Frank Candocia[*], Malek Adjouadi[*]

Prasanna Jayakar[+], and Ilker Yaylali[+]

[*] Department of Electrical and Computer Engineering, Florida International University, http://www.fiu.edu, USA
[+] Neuroscience Center, Miami Children's Hospital, http://www.mch.com, USA

ABSTRACT

This paper describes an intensity-based image registration algorithm using the affine transformation. The images considered are Single Photon Emission Computed Tomography (SPECT) brain images provided by the Neuroscience group at Miami Children's Hospital. Registration must be performed on time-series images for which any meaningful pixel-to-pixel comparisons will be made. This is done so that the images are brought into spatial alignment and made to share a common coordinate system. It will be demonstrated that the algorithm implemented here gives comparable results to those obtained from an image registration program currently in clinical use, and yet utilizes a less constrained mathematical approach. The basis of the clinical registration program is the AIR (Automated Image Registration) software package designed by Roger Woods and colleagues at the UCLA Medical School. The comparisons made between the registration results obtained from the affine algorithm and the commercial package will be demonstrated visually with 3-D rendered graphics and numerically by the use of mean square error. It will be argued that even though the rigid-body transformation is often suggested for intra-modality medical image registration, the affine transformation is a more general mathematical solution to the misalignment problem that gives comparable results without the additional complexity.

KEY WORDS

Affine Transformation, SPECT, Registration, Medical Images

1. Introduction

The ultimate focus of this research concerning brain images is placed on the detection and accurate localization of epileptic foci using non-invasive imaging techniques. To this end, SPECT images are used routinely for the non-invasive visualization of human brain function. These images often serve an indispensable role in the pre-surgical diagnosis and localization of neurological dysfunctions. In the specific case of epilepsy surgery, the imaging capabilities provided through the integration of SPECT, MRI (Magnetic Resonance Imaging), fMRI (functional MRI), and EEG (electro-encephalogram) are used to provide the surgeon with an accurate depiction of the in-vivo neurology, allowing the visualization of vascular malformations, lesions, and abnormal perfusion and electrical patterns existing in the tissues of the brain [1]. In order to maximize the information presented by each imaging modality, image registration is viewed as an essential task. Toward achievement of useful multi-modality imaging studies, it has been argued that intra-modality registration (SPECT-to-SPECT) is more critical than that of the inter-modality (SPECT-to-MRI) [2]. That is, errors in pre-surgical localization of dysfunctions are attributed mostly to poor SPECT registration. To this end, accurate intra-modality registration must be applied to images created through multiple SPECT scanning sessions prior to their overall incorporation into the integrated brain study. Since SPECT only provides static images of an organ, multiple SPECT studies (a time-series) must be created in order to accentuate the dynamics of the organ.

Specifically, many researchers have agreed that epileptic foci are reliably localized with a subtraction SPECT image [3,4]. This image is created via the information from two registered studies, where one study depicts normal, non-epileptic brain function (interictal SPECT) and the other depicts the brain during the epileptic event (ictal SPECT). Subtraction accentuates the changes in cerebral blood flow (perfusion); regions of the brain that undergo large changes in perfusion are cited as "probable" epileptic foci by medical experts [5]. Based on these considerations, the emphasis of this publication will be placed on intra-modality registration of time series SPECT images.

Given the importance of such a research focus and its practical implications, accurate image registration is essential in providing the desired outcome. The choice of registration algorithm is often not simple to make, as many criteria must be considered. Obviously, the ultimate merit of any algorithm is gauged by the

correctness of the results it provides. However, in a practical setting, it is advantageous that the method of registration be not only accurate, but also should be automatic (not requiring human intervention), time efficient, and robust, giving reliable results even when noisy, low resolution images are encountered. Thus, the complexity of the registration method is a function of the details of the problem addressed and its anticipated results.

2. Types Of Image Registration

Several registration methods have been implemented for use with medical images. Feature based registration algorithms have been employed in the past for medical image registration [6]. These methods have been used with acceptable results, but their success is subject to constraints. Feature based registration involves the use of extracted anatomical references from images. After the features are segmented from the data sets, a geometric transformation would need to be found that aligns the pixels representing these corresponding features (surfaces, contours, etc.) in the pair of images. This set of transformation coefficients could then be applied to the two complete image datasets to register them. Though this method has some merits, it also has deficiencies. Often, the significant features in medical image data are small, distinct regions, each occupying only a small fraction of the total dataset size. Thus, a reduced amount of image data could be used in the calculation of the transformation coefficient matrix; this leads to a more computationally efficient registration procedure. Shortcomings of this method are that it is not automatic since it requires intervention by a user familiar with the relevant anatomy in order to identify the pertinent features that will be used for matching [7]. Additionally, SPECT images inherently have low resolution and poorly defined contours, making them difficult to segment. Thus, feature based registrations for SPECT studies must contend with such subtle aspects [8].

On the other hand, registrations based on pixel-intensity techniques have been more successful. Many are based on the 3-D rigid-body transformation; most researchers who justify its use as a sufficient registration solution argue that the brain is basically a non-deformable organ and that translation plus pure rotations can effectively correct the geometric misalignments between two studies [9]. It can also be shown that this method is robust to noise. It can be argued, however, that the registration based on the rigid body constraint is not sufficient to completely correct for the misalignments between two SPECT brain studies. Rigid body registration does not allow for any component of the registration to correct for misalignments caused by the perspective (shearing) effects. In support of these assertions, descriptions and comparisons of results from both algorithms, affine and rigid body, will be explicitly described in the following sections.

3. Mathematical Description of the Affine Transformation

An affine transformation can be described as any transformation that preserves co-linearity and ratios of distances between the points of a data set. The affine transformation of $\Re^n$ is a mapping F: $\Re^n \rightarrow \Re^n$ of the form:

$$F(p) = Ap + q \tag{1}$$

where p,q$\in \Re^n$ and A is a linear transformation of $\Re^n$. Note that a nonsingular map A: $\Re^n \rightarrow \Re^n$ is orientation preserving if det(A) > 0 and orientation reversing when det(A) < 0. In a 2-D space, the affine transformation between point pair $\underline{x}$' and $\underline{x}$ is given by:

$$\begin{bmatrix} x' \\ y' \end{bmatrix} = \begin{bmatrix} a_{11} & a_{12} \\ a_{21} & a_{22} \end{bmatrix} \bullet \begin{bmatrix} x \\ y \end{bmatrix} + \begin{bmatrix} b_1 \\ b_2 \end{bmatrix} \tag{2}$$

Note that the affine transformation is a combination of several mathematical operations; namely, these are: rotation, scaling, translation, reflection, and shear [10]. On the other hand, a special, constrained case of the affine transformation exists, known as the Euclidean, or rigid-body, transformation. For this case, A will be formulated as:

$$A = \begin{bmatrix} \cos(\theta) & \sin(\theta) \\ -\sin(\theta) & \cos(\theta) \end{bmatrix} \tag{3}$$

This type of transformation defines a pure rotation along with a translation (all other operations are nullified) and A must be constrained mathematically so that det(A) ≡ 1. It is important to note that the affine transformation does not constrain the values of the matrix A in this way.

4. Mathematical Assumptions

The process of registration involves some examination of the two sets of data in order to determine a mathematical correspondence (a set of transformation coefficients) that will bring the image pair into spatial alignment. In general, a registration routine is determined by the selection of three components [11]. Namely, these are:

1. Feature space, or the data subset extracted for the purpose of matching
2. Similarity measure, or the numerical figure which will be used to assess the quality of the registration
3. Search space, or the set of permutations within which exists the most optimal solution matrix

Firstly, since an intensity-based transform is desired, the feature space will be the entire set of pixels for both images. This suggests that no prior assumptions about the datasets will be made. Relating to the second component, common similarity measures chosen are mean square error, optical flow error, sum of variances, and normalized entropy [11]. For this implementation, the optical flow error will be chosen as the similarity measure. The success of the registration procedure will depend on the minimization of the similarity measure. The rationale for these considerations will be discussed in the next section. Lastly, the search space becomes dependent on the mathematical model chosen for the registration (i.e. the number of degrees of freedom considered).

5. Brightness Constraint

It is often assumed that images taken over short time intervals Δt have smoothly varying optical flows. Specifically, it is assumed that the irradiance E(x,y,t) at time t at image point (x,y) will be equal to the irradiance at time $t+\delta t$ at the image point $(x+u\cdot\delta t, y+v\cdot\delta t)$, where u and v are the x and y components of the optical flow vector at that point [12]. This well known relation is formulated as such:

$$E(x+u\delta t, y+v\delta t, t+\delta t) = E(x,y,t) \tag{4}$$

If brightness varies smoothly, a Taylor series expansion can be performed to expand the above equation:

$$E(x,y,t)+\delta x\cdot\frac{\partial E}{\partial x}+\delta y\cdot\frac{\partial E}{\partial y}+\delta t\cdot\frac{\partial E}{\partial t}+e=E(x,y,t) \tag{5}$$

Canceling E(x,y,t) terms, dividing the remainder by δt, assuming that the '*e*' term represents the negligible contribution of higher order terms in δx, δy, and δt, and taking the limit as $\delta t \to 0$ gives:

$$\frac{\partial E}{\partial x}\cdot\frac{dx}{dt}+\frac{\partial E}{\partial y}\cdot\frac{dy}{dt}+\frac{\partial E}{\partial t}=0 \tag{6}$$

Based on the brightness constraint, it may be assumed that the relative motion between two images may be estimated via a least-squares minimization of the optical flow error [13]. Therefore, the following error function will be minimized:

$$Eflow=\sum_{\underline{x}}\left[\underline{U}_m^{\,T}\,E_{\underline{x}}+E_t\right]^2 \tag{7}$$

$$where\ \underline{U}_m=\underline{x}'-\underline{x}=\begin{bmatrix}x'\\y'\end{bmatrix}-\begin{bmatrix}x\\y\end{bmatrix}\quad and\quad \underline{x}'=\underline{A}\underline{x}+\underline{b}$$

6. Structure of the Algorithm Based on the Affine Transformation

The algorithm developed in this study takes strength from its general, unconstrained approach to the problem of image registration. For the case of images produced through intra-patient SPECT, it is anticipated that the affine algorithm will produce accurate registration results. Mathematically, the affine equation is a coordinate transformation that is described by the following formulation:

$$\underline{x}'=\underline{A}\underline{x}+\underline{b} \tag{8}$$

This transformation can be extended to 3 dimensions but is more concisely described for the 2-D case. For the 2-D case, the matrix form of the transformation, given in Equation 8, yields:

$$\begin{bmatrix}x'\\y'\end{bmatrix}=\begin{bmatrix}a_{11}&a_{12}\\a_{21}&a_{22}\end{bmatrix}\bullet\begin{bmatrix}x\\y\end{bmatrix}+\begin{bmatrix}b_1\\b_2\end{bmatrix} \tag{9}$$

The axes of image #2 (x' and y') are considered as a rotated and translated version of the axes of image #1 (x and y), where the coefficients of matrix $\underline{A}$ denote a rotational transformation and the coefficients of matrix $\underline{b}$ denote a translation offset. Based on the earlier assumptions made in Section 5, the optical flow error may be expanded as follows:

$$\mathrm{E}flow=\sum_{\underline{x}}\left[\left(\underline{A}\underline{x}+\underline{b}-\underline{x}\right)^T\underline{E}_x+E_t\right]^2$$

$$\mathrm{E}flow=\sum_{\underline{x}}\left[\left(F1\right)E_x+\left(F2\right)E_y+E_t\right]^2 \tag{10}$$

$$F1=(a_{11}-1)x+a_{12}\cdot y+b_1$$

$$F2=a_{21}\cdot x+(a_{22}-1)y+b_2$$

In short form, E_{flow} can be rewritten as:

$$\mathrm{E}flow=\sum_{\underline{x}}\left[\Psi\right]^2 \tag{11}$$

To minimize the optical flow error, the partial derivatives of the function must be taken with respect to each parameter for which the transformation depends and then equated to zero. These parameters are a_{11}, a_{12}, a_{21}, a_{22}, b_1, and b_2. The following system of equations is thus established:

$$\frac{\partial E_{flow}}{\partial a_{11}} = 2\sum_{\underline{x}}[\Psi][x \cdot E_x] = 0$$
$$\frac{\partial E_{flow}}{\partial a_{12}} = 2\sum_{\underline{x}}[\Psi][y \cdot E_x] = 0$$
$$\frac{\partial E_{flow}}{\partial b_1} = 2\sum_{\underline{x}}[\Psi][E_x] = 0$$
$$\frac{\partial E_{flow}}{\partial a_{21}} = 2\sum_{\underline{x}}[\Psi][x \cdot E_y] = 0$$
$$\frac{\partial E_{flow}}{\partial a_{22}} = 2\sum_{\underline{x}}[\Psi][y \cdot E_y] = 0$$
$$\frac{\partial E_{flow}}{\partial b_2} = 2\sum_{\underline{x}}[\Psi][E_y] = 0 \qquad (12)$$

To simplify the solution of this system, shorthand notations are used in the following way:

$$\Phi = \begin{bmatrix} xE_x & yE_x & E_x & xE_y & yE_y & E_y \end{bmatrix}^T$$
$$C = \begin{bmatrix} a_{11} & a_{12} & b_1 & a_{21} & a_{22} & b_2 \end{bmatrix}^T \qquad (13)$$

The optical flow error equation can then be written more succinctly as follows:

$$E_{flow} = \sum_{\underline{x}} \left[\Phi^T C - xEx - yEy + Et \right]^2 \qquad (14)$$

Therefore, the partial derivatives calculated previously can be rewritten as follows:

$$\sum_{\underline{x}} [\Phi^T C][xEx] = \sum_{\underline{x}} [xEx + yEy - Et][xEx]$$
$$\sum_{\underline{x}} [\Phi^T C][yEx] = \sum_{\underline{x}} [xEx + yEy - Et][yEx]$$
$$\sum_{\underline{x}} [\Phi^T C][Ex] = \sum_{\underline{x}} [xEx + yEy - Et][Ex]$$
$$\sum_{\underline{x}} [\Phi^T C][xEy] = \sum_{\underline{x}} [xEx + yEy - Et][xEy]$$
$$\sum_{\underline{x}} [\Phi^T C][yEy] = \sum_{\underline{x}} [xEx + yEy - Et][yEy]$$
$$\sum_{\underline{x}} [\Phi^T C][Ey] = \sum_{\underline{x}} [xEx + yEy - Et][Ey] \qquad (15)$$

Again simplifying, gives:

$$\sum_{\underline{x}} [\Phi \cdot \Phi^T \cdot C] = \sum_{\underline{x}} [xEx + yEy - Et][\Phi] \qquad (16)$$

Ultimately, solving for matrix C yields:

$$\begin{bmatrix} a11 \\ a12 \\ b1 \\ a21 \\ a22 \\ b2 \end{bmatrix} = \left[\sum_{\underline{x}} \Phi\Phi^T\right]^{-1} \left[\sum_{\underline{x}} (xEx + yEy - Et)(\Phi)\right] \qquad (17)$$

7. Results

Registration performed through use of the 3-D affine transformation can be shown to be comparable to that provided by the 3-D rigid body transformation. For the purposes of visualization, the Matlab software package was used to provide rendered surface images of each SPECT image. For the experimental tests of the algorithms, ictal and interictal HMPAO SPECT studies, each consisting of 40 transaxial slices of 128x128 pixel, 16-bit resolution images, were used. Figures 1a – 1c and 2a – 2b demonstrate the improvement in image spatial alignment provided by the affine implementation.

When the figures 1a and 1b (unregistered images) are viewed, it is noticeable that they do not share the same physical orientation. This is best exemplified by noting the reference planes on the top of each data set. For images 1a and 1b, these planes are not parallel. Note that between Figure 1a and 1c (registered images) these planes become appropriately oriented. A similar effect is noted for the rigid body registration result (Figure 1d).

A comparison between the affine and rigid-body registrations with regards to overall mean square error was made. When the mean square error between the unregistered image pair was computed, its value was 3.4334×10^4. Mean square error between the affine registered pair produced a value of 1.5192×10^3; likewise, the mean square error produced from the rigid-body registered pair, performed using the AIR software, was 1.6724×10^3. These numbers are large due to the fact there are often large differences in pixel gray scales between SPECT studies, even with optimal registration.

By observing the 3-D scatter plot in figure 2a, it should become apparent that the image pair had a visible misalignment before registration. The image is a depiction of the volume of pixels that do not correspond prior to registration. This volume percentage (number of pixels unregistered divided by total number of pixels in the two studies) is quite large (29.27%). After registration, it is observed that this volume of pixels is significantly reduced. After registration, the volume percentages are 4.87% and 4.75% for affine and rigid-body registrations, respectively. These results can be visualized by observing figures 2b and 2c. In summation, it can be inferred that the results obtained from the affine registration algorithm are virtually identical to those obtained through the use of the rigid-body registration.

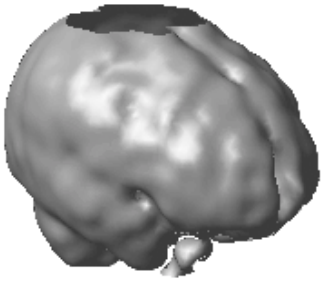

Figure 1a: ictal image (reference image)

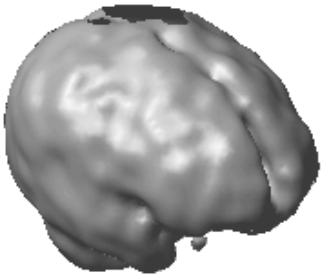

Figure 1b: interictal image before registration

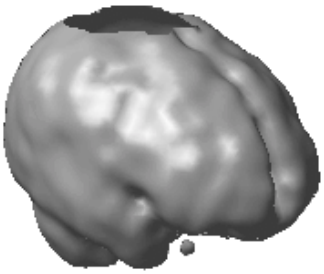

Figure 1c: interictal image after using affine registration

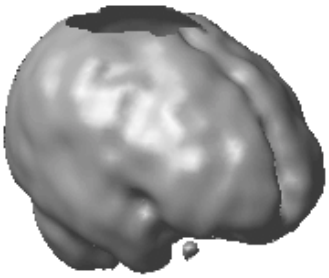

Figure 1d: interictal image using commercially-available rigid-body registration

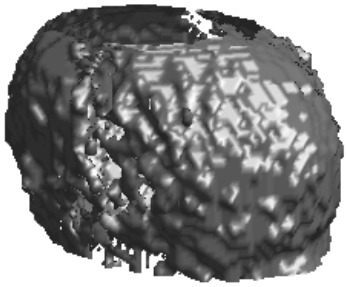

Figure 2a: scatter plot of the unregistered volume

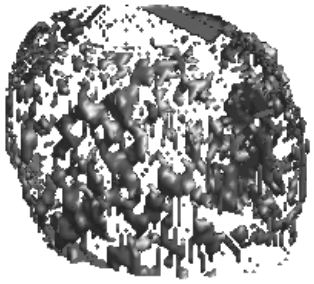

Figure 2b: scatter plot of residual volume after affine registration

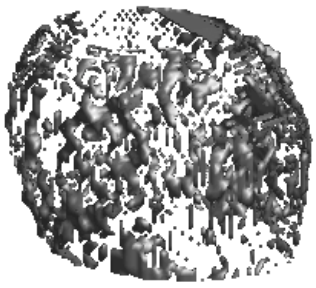

Figure 2c: scatter plot of residual volume after rigid body registration

8. Conclusion

The premise for developing this algorithm was to overcome critical constraints imposed by the nature of SPECT images. The objective was to develop a mathematical framework that overcame the burden of co-registering pairs of images, albeit in an intra-modality platform, subject to the unknown experimental conditions that led to the misalignments, just as we contended with the issues of low resolution and the effects of noise.

The choice in using the affine transformation was considered with direct regards to such concerns, and its implementation proved, through the obtained results, that it shows great promise in terms of its real-world implications. These results, shared with our medical colleagues, generated the enthusiasm to proceed with additional data gathered from several patients.

The contribution of such work is in defining that the affine transformation does compare in its results to a commercially available software package. In so doing, we are now positioned to refine the mathematics and will be able to address different experimental situations while not restricting ourselves to a software package that is fixed by its specific mathematical disposition.

Acknowledgments

We wish to thank the National Science Foundation and the Office of Naval Research for their support under grants EIA-9906600 and N-000149910952.

References

[1] A.S. Harvey, Temporal lobe epilepsy in childhood, Ph.D. Thesis, University of Melbourne, 1993.

[2] B.H. Brinkmann, T.J. O'Brien, J. Terence, B.P. Mullan, M.K. O'Connor, R.A. Robb, and E.L. So, Subtraction ictal SPECT coregistered to MRI for seizure focus localization in partial epilepsy, *Mayo Clin Proc*, *75*(6), 2000, 615-624.

[3] T.J. O'Brien, E.L. So, B.P. Mullan, M.F. Hauser, B.H. Brinkmann, N.I. Bohnen, D. Hanson, G.D. Cascino, C.R. Jack, Jr. and F.W. Sharbrough, Subtraction ictal SPECT co-registered to MRI improves clinical usefulness of SPECT in localizing the seizure surgical focus, *Neurology*, *50*(2), 1998, 445-455.

[4] H.W. Lee, S.B. Hong and W.S. Tae, Opposite ictal perfusion patterns of subtracted SPECT, *Brain*, *123*, 2000, 2150-2159.

[5] R.A. Avery, I.G. Zubal, R. Stokking, C. Studholme, M. Corsi, J.P. Seibyl and S.S. Spencer, Decreased cerebral blood flow during seizures with ictal SPECT injections, *Epilepsy Research*, *40*, 2000, 53-61.

[6] J.B.A. Maintz and M.A. Viergever, A survey of medical image registration, *Medical Image Analysis*, *2*(1), 1998, 1-37.

[7] R.P. Woods, S.R. Cherry and J.C. Mazziota, Rapid automated algorithm for aligning and reslicing PET images, *Journal of Computer Assisted Technology*, *16*(4), 1992, 620-633.

[8] J. Feldmar, G. Malandain, J. Declerck and N. Ayache, Extension of the ICP algorithm to non rigid intensity-based registration of 3-D volumes, *Computer Vision and Image Understanding*, *66*(2), 1997, 193-206.

[9] R.P. Woods, Within-modality registration using intensity-based cost functions, in I. Bankman (Ed.) *Handbook of Medical Imaging: Processing and Analysis*, 33 (New York: Academic Press, 2000).

[10] Z. Yang and F.S. Cohen, Image registration and object recognition using affine invariants and convex hulls, *IEEE Trans. Image Processing*, *8*(7), 1999, 934-946.

[11] L.G. Brown, A survey of image registration techniques, *ACM Computing Surveys*, *24*(4), 1992, 325-376.

[12] B.K.P. Horn, *Robot Vision* (New York: McGraw-Hill, 1986) 278-293.

[13] S. Mann and R.W. Picard, Video orbits of the projective group: a simple approach to featureless estimation of parameters, *IEEE Trans. Image Processing*, *6*(9), 1997, 1281-1295.